Activin/Smad2 and Wnt/β-catenin up-regulate HAS2 and ALDH3A2 to facilitate mesendoderm differentiation of human embryonic stem cells

Received for publication, April 24, 2018, and in revised form, September 6, 2018 Published, Papers in Press, October 3, 2018, DOI 10.1074/jbc.RA118.003688

Xuanhao Xu[‡1], **Lu Wang**[‡1], **Bofeng Liu**[§], **Wei Xie**[§], **and Ye-Guang Chen**[‡2]

From the [‡]*State Key Laboratory of Membrane Biology, Tsinghua-Peking Center for Life Sciences, School of Life Sciences, Tsinghua University, Beijing 100084 and the* [§]*Tsinghua-Peking Center for Life Sciences, School of Life Sciences, Tsinghua University, Beijing 100084, China*

Edited by Alex Toker

Activin and Wnt signaling are necessary and sufficient for mesendoderm (ME) differentiation of human embryonic stem cells (ESCs). In this study, we report that during ME differentiation induced by Activin and Wnt, Activin/Smad2 induces a decrease of the repressive histone modification of H3K27me3 by promoting the proteasome-dependent degradation of enhancer of zeste 2 polycomb (EZH2)-repressive complex 2 subunit. As a result, recruitment of the forkhead protein FOXH1 on open chromatin regions integrates the signals of Activin/Smad2 and Wnt/β-catenin to activate the expression of the ME genes including *HAS2* and *ALDH3A2*. Consistently, H3K27me3 decrease is enriched on open chromatin around regulatory regions. Furthermore, knockdown of *HAS2* or *ALDH3A2* greatly attenuates ME differentiation. These findings unveil a pathway from extracellular signals to epigenetic modification–mediated gene activation during ME commitment.

Differentiation of embryonic stem cells (ESCs)[3] into a specific lineage involves the finely tuned coordination between extrinsic signals and intrinsic mediators (1, 2). Among extrinsic factors, TGF-β (transforming growth factor-β) and Wnt signals have been shown to be critical in mesendoderm (ME) specification (3–12). The TGF-β superfamily members Activin/Nodal play a vital role in mesendoderm differentiation during gastrulation (13). Through phosphorylation by the Activin/Nodal receptors, Smad2/3 are activated and then work with Smad4 to regulate gene expression in the nucleus (14–17). The canonical Wnt/β-catenin pathway regulates a variety of cellular events such as cell proliferation, differentiation, and migration and controls embryo patterning (18, 19).

Chromatin accessibility of genes that determine cell fates is modulated by various factors including epigenetic modifiers and chromatin remodelers (2, 11, 13, 20). The inactive or active state of chromatin can be robustly maintained through the cross-talk among different histone modifications. H3K27ac is characterized for open chromatin and actively transcribed genes, whereas trimethylation of histone H3 on lysine 27 (H3K27me3) is a repressive mark linked to silent chromatin and gene repression (21–24). Whole-genome studies have revealed that H3K27me3 occupies critical developmental genes in both human and mouse embryonic stem cells, and often coexists with the active mark H3K4me3, forming a poised state at regulatory regions of differentiation genes (25, 26). Chromatin accessibility depends on the overall effects of those histone modifications upon differentiation of signal stimulation (22). Although open chromatin signals have been reported to be associated with ME, endoderm, and mesoderm differentiation (27), it is unclear how open chromatin is linked to histone modifications and transcription at the early stage of ME differentiation.

Our previous work demonstrated that during ME specification, Activin decreases H3K27me3 levels via the Smad2-mediated reduction of the EZH2 protein, the methyltransferase subunit of polycomb repressive complex 2 (PRC2) (11). To test whether decreased H3K27me3 would result in elevated chromatin accessibility in the early stage of Activin and Wnt-induced ME differentiation, we applied the assay for transposase-accessible chromatin with a high-throughput sequencing (ATAC-seq) approach to assess accessible chromatin. We found that, although Activin stimulation could not alter global open chromatin, the decreased H3K27me3 modification at the transcription start site (TSS) regions elevates chromatin accessibility and thus facilitates the recruitment of β-catenin. Then Smad2 and β-catenin, together with other factors such as FOXH1, activate gene expression to ensure ME specification. From the Activin and Wnt-co-regulated genes, we further found that hyaluronan synthase 2 (*HAS2*) and aldehyde dehydrogenase 3 family member A2 (*ALDH3A2*), which are regulated by Smad2–β-catenin–FOXH1, are critical for ME differentiation.

This work was supported by National Natural Science Foundation of China Grant 31730056 and National Key Research and Development Program of China Grant 2017YFA0103601 (to Y. G. C.). The authors declare that they have no conflicts of interest with the contents of this article.

This article contains Tables S1–S6.

The ATAC-sequence data for this study were deposited to the Gene Expression Omnibus (GEO) database under GEO accession number GSE113047.

[1] Both authors contributed equally to this work.

[2] To whom correspondence should be addressed. E-mail: ygchen@tsinghua.edu.cn.

[3] The abbreviations used are: ESC, embryonic stem cell; ME, mesendoderm; ALDH3A2, aldehyde dehydrogenase 3 family member A2; ChIP-seq, chromatin immunoprecipitation sequencing; HAS2, hyaluronan synthase 2; PRC2, polycomb repressive complex 2; TGF-β, transforming growth factor-β; RA, retinoic acid; DMEM, Dulbecco's modified Eagle's medium; TSS, transcription start site; bFGF, basis fibroblast growth factor; shRNA, short hairpin RNA; qPCR, quantitative PCR; GAPDH, glyceraldehyde-3-phosphate dehydrogenase; EZH2, enhancer of zeste 2 polycomb RPKM, reads per kilobase of bin per million.

Results

Smad2 and β-catenin binding motifs are enriched in the open promoter regions of ME markers

We have previously demonstrated that Activin A and Wnt3a could efficiently induce ME differentiation of human ESCs, and Activin A reduced H3K27me3 levels in the early stage of ME commitment (11). As H3K27me3 has been shown to associate with chromatin accessibility (24, 28), we attempted to investigate whether open chromatin was changed during AW-induced ME differentiation. To this end, we performed ATAC-seq with human H1 ESCs upon treatment of 25 ng/ml of Activin A, 25 ng/ml of Wnt3a, or both (AW) for 6 h, but found no significant global open region changes at the early stage of mesendoderm differentiation (Fig. 1*A*). After analyzing the distribution of those open signals, we found a large percentage of open peaks were enriched around TSS regions (Fig. 1*B*). In addition, comparing gene expression profiles from the published RNA-seq data (11), we found that although open regions showed little change in the promoters of different lineage genes upon 6 h treatment of AW, the expression of ME genes was up-regulated, whereas no obvious changes in pluripotency, neuroectoderm, or trophoblast markers (Fig. 1*C*, Table S1), indicating that open chromatin does not ensure gene expression and lineage determination, and other regulatory events should exist to determine ME differentiation.

By analyzing the published ChIP-sequencing (ChIP-seq) data of Smad2, H3K27me3, H3K4me3 (GSE81617) (11), β-catenin, and RNA polymerase II (GSE64758) (10), in combination with our ATAC-seq data (GSE113047), we found that AW-induced Smad2 binding was overlapped with the open chromatin regions around TSS of the ME markers such as *T*, *EOMES*, *FGF8*, and *WNT3* (Fig. 1*D*). ChIP-PCR analysis supported that Smad2 and β-catenin bound on the regulatory regions of *T*, *EOMES*, and *FGF8* after AW treatment (Fig. 1*E*). Interestingly, the open regions coincided with the AW-induced H3K27me3 decrease and RNA polymerase II binding in these ME genes. Moreover, Wnt-induced β-catenin binding was well-overlapped with these regions, consistent with the cooperation of Smad2 and β-catenin to activate transcription of mesendoderm genes. Smad2 and β-catenin co-occupied the regulatory regions of the pluripotency genes *OCT4* and *SALL4*, but they were not detected in the regulatory regions of the ectoderm gene *SOX1* and the trophoblast gene *CGA* (Fig. 1, *F* and *G*).

EZH2 degradation is responsible for Activin/Smad2-induced H3K27me3 decrease

Next we explored the relationship of histone modifications and chromatin opening during ME specification at the genome-wide level. As shown in Fig. 2*A*, there was a close overlap between decreased H3K27me3 modification and open chromatin signals at about ±2.5k of TSS after AW treatment, whereas the H3K4me3 level showed little change.

It has been shown that EZH2 plays a critical role in maintaining H3K27me3 levels during ME differentiation (11, 29). To further confirm the role of Activin/Smad signaling in modulating H3K27me3 levels, we knocked down *Smad2* in H1 cells (Fig. 2*B*), and found that *Smad2* depletion did not change the expression of the pluripotency genes *OCT4* and *NANOG* (Fig. 2*C*). In agreement with our early report (11), AW reduced the levels of H3K27me3 and EZH2, and depletion of *Smad2*, but not *β-catenin*, blocked the AW-induced reductions (Fig. 2*D*). Furthermore, Activin-induced EZH2 ubiquitination was decreased by *Smurf2* knockdown (Fig. 2*E*), and the proteasome inhibitor MG132 attenuated AW-induced EZH2 degradation (Fig. 2*F*). In line with it, the proteasome inhibitors MG132 and bortezomib, but not the lysosome inhibitor bafilomycin A, blocked Activin-induced EZH2 degradation (Fig. 2*G*). These data together suggest that Activin/Smad2 signaling promotes EZH2 degradation through the proteasome pathway, reduces H3K27me3 modification, and thus alters the balance of H3K27me3-H3K4me3 in the open chromatin regions.

Smad2 decreases H3K27me3 independent of Smad4

As Smad2 has weak DNA binding ability and Smad2 cooperates with Smad4 to regulate transcription (14–16), we wondered whether the Smad2-mediated H3K27me3 decrease depends on Smad4. Transient depletion of *Smad4* did not affect pluripotency gene expression but greatly impaired AW-induced ME differentiation (Fig. 3, *A* and *B*). Although knockdown of *Smad4* dramatically reduced enrichment of Smad2 on ME genes (Fig. 3*C*), it had no impact on the Activin/Smad2-induced decrease of H3K27me3 and EZH2 (Fig. 3*D*). Together these data indicate that Smad4 is dispensable for Smad2-mediated H3K27me3 and EZH2 decrease, but is critical for Smad2 to bind to ME marker genes and contributes to ME differentiation.

Smad2 and β-catenin cooperate with FOXH1 to promote ME differentiation

To explore the possible recruitment of transcription factors to the open chromatin regions, we picked up the top 200 enriched binding motifs of transcription factors in the open chromatin regions upon AW treatment and focused on those involved in lineage determination. Among them, the binding motifs of the mesenderm- or endoderm-related factors (ME: EOMES and T; endoderm: SOX17, FOXA2, and FOXH1) were strongly enriched (Fig. 4*A*), whereas the ectoderm (PAX6, SOX1, OLIG1) or trophoblast markers (GATA3, CDX2) were not (data not shown). EOMES and T not only serve as ME markers, but also are the critical regulators for ME fate determination (30, 31), suggesting that the open chromatin state provides the accessibility of ME lineage regulators at the early stage of ME differentiation.

As enrichment of the binding motifs for Smad2/Smad3 and T cell factor 4 (TCF4) was also observed, we asked whether knockdown of *Smad2* would influence β-catenin binding to the ME gene promoters. As shown in Fig. 4*B*, the AW-induced occupancy of β-catenin was abolished in *Smad2* knockdown cells. As Smad2 mediates the transcription state by promoting EZH2 degradation and reducing H3K27me3 levels, we tested whether the EZH2 inhibitor DZNep could mimic the function of Activin/Smad2 to enhance β-catenin binding to ME gene promoters. Treatment using 25 ng/ml of Wnt3a for 6 h slightly increased β-catenin enrichment on the ME genes *T*, *EOMES*, and *FGF8*, but pretreatment of DZNep for 2 h apparently

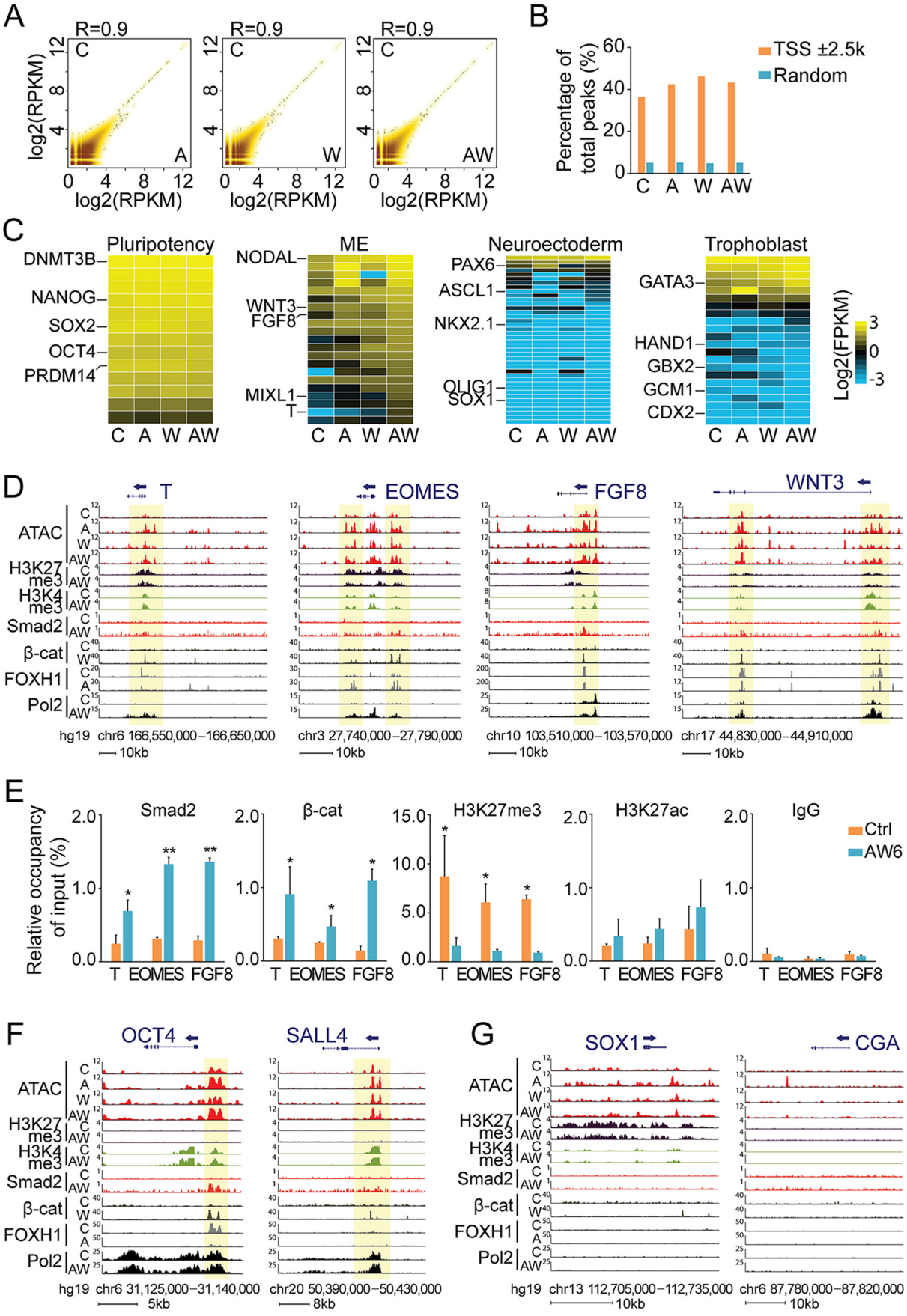
A
R=0.9
C
A
W
AW
log2(RPKM)
B
Percentage of total peaks (%)
TSS ±2.5k
Random
C
Pluripotency
DNMT3B
NANOG
SOX2
OCT4
PRDM14
ME
NODAL
WNT3
FGF8
MIXL1
T
Neuroectoderm
PAX6
ASCL1
NKX2.1
OLIG1
SOX1
Trophoblast
GATA3
HAND1
GBX2
GCM1
CDX2
Log2(FPKM)
D
T
EOMES
FGF8
WNT3
ATAC
H3K27 me3
H3K4 me3
Smad2
β-cat
FOXH1
Pol2
hg19 chr6 166,550,000–166,650,000
chr3 27,740,000–27,790,000
chr10 103,510,000–103,570,000
chr17 44,830,000–44,910,000
10kb
E
Relative occupancy of input (%)
Smad2
β-cat
H3K27me3
H3K27ac
IgG
Ctrl
AW6
T EOMES FGF8
F
OCT4
SALL4
hg19 chr6 31,125,000–31,140,000
chr20 50,390,000–50,430,000
5kb
8kb
G
SOX1
CGA
hg19 chr13 112,705,000–112,735,000
chr6 87,780,000–87,820,000
10kb

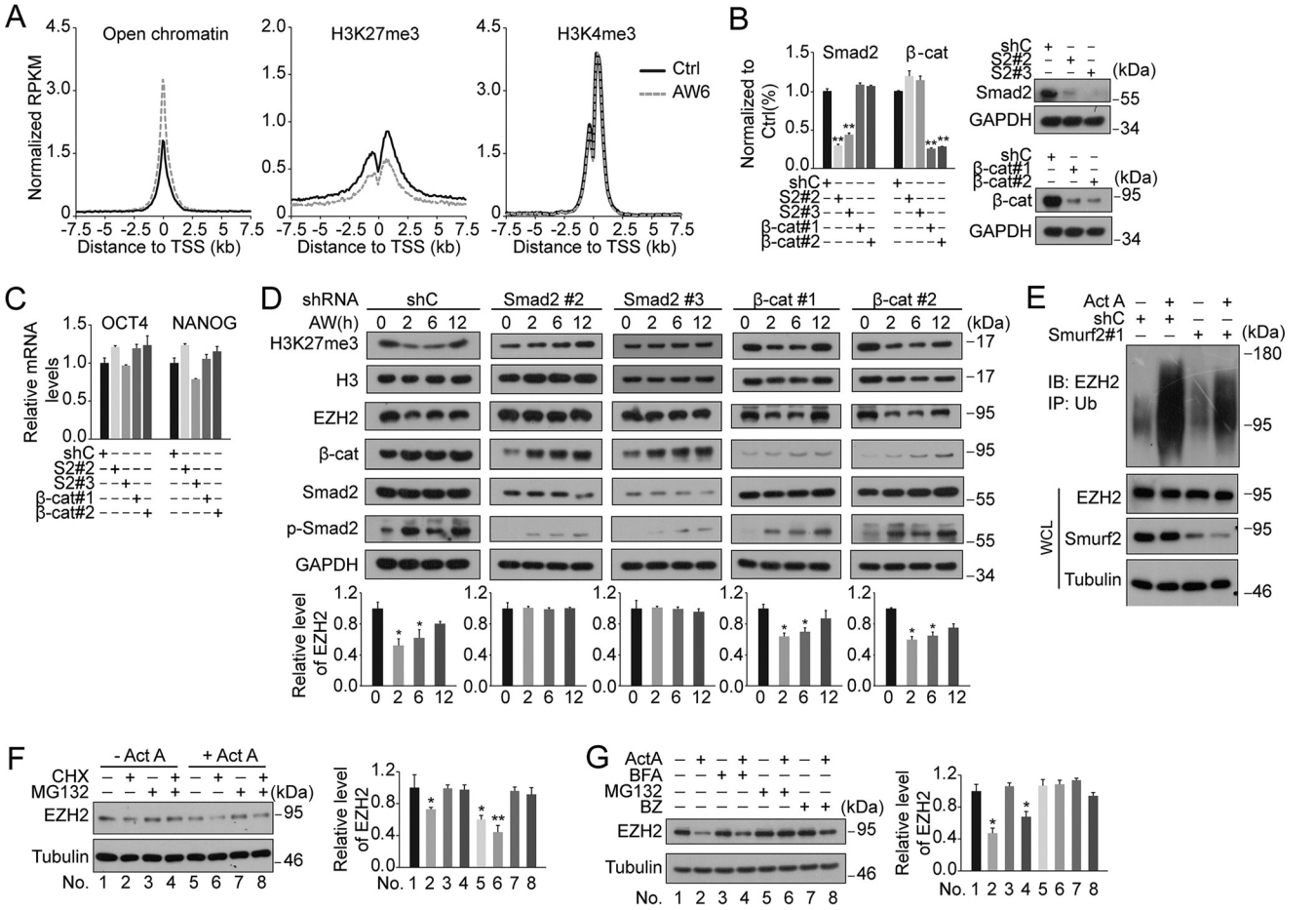

Figure 2. Activin/Smad2 signaling promotes EZH2 degradation. *A*, genome-wide analysis shows that decreased H3K27me3 was related with open chromatin regions at about ±2.5k of TSS after AW treatment. *B*, H1 cells transfected with control or shRNA and collected for qPCR and immunoblotting. *C*, pluripotent markers were measured by qPCR in *Smad2* or *β-catenin* knockdown cells. *D*, *Smad2* or *β-catenin*-knockdown H1 cells were treated with 25 ng/ml of AW for the indicated times before harvested for histone extraction and then anti-H3K27me3 immunoblotting. The whole cell lysate was used for immunoblotting with the indicated antibodies. GAPDH served as loading control. *E*, after pre-treatment with 5 μg/ml of MG132 for 2 h, *Smurf2*-knockdown cells were treated with 25 ng/ml of Activin A for 2 h, and subjected for anti-ubiquitin immunoprecipitation followed by anti-EZH2 immunoblotting. *F*, H1 cell were treated with 10 μg/ml of cycloheximide (*CHX*), 5 μg/ml of MG132 or both in the presence or absence of 25 ng/ml of Activin A for 2 h, and then harvested for anti-EZH2 immunoblotting. *G*, H1 cell were treated with 0.1 μM bafilomycin A1 (*BFA*), 5 μg/ml of MG132 or 0.05 μM bortezomib (*BZ*) in the presence or absence of 25 ng/ml of Activin A for 2 h, and then harvested for anti-EZH2 immunoblotting. The relative level of EZH2 was shown after normalized to tubulin, and statistical data were shown as mean ± S.E. by unpaired, two-tailed Student's *t* test ($n = 3$, including 3 biological replicates). *, $p < 0.05$; **, $p < 0.01$.

enhanced Wnt3a-induced β-catenin binding (Fig. 4*C*). These data indicate that Activin/Smad2-altered histone modification is required for β-catenin recruitment to ME genes. Furthermore, knockdown of either *Smad2* or *β-catenin* greatly impaired expression of ME markers (Fig. 4*D*), indicating that cooperation of Smad2 and β-catenin is critical for AW-induced ME differentiation.

The binding motif of *FOXH1* was also enriched by Activin treatment (Fig. 4*B*). It has been shown that FOXH1 interacts with Smad2 and is required for Activin responses during early embryonic patterning (32–36). Consistently, *FOXH1* knockdown dampened ME differentiation (Fig. 4*E*). By analyzing the FOXH1 ChIP-seq data (GSE29422) (37), we found that its binding pattern overlaps with Smad2 and β-catenin in the regulatory regions of the ME genes, but not in the ectoderm or trophoblast genes (Fig. 1, *D*, *F*, and *G*). Although FOXH1 interacted only with Smad2 but not with TCF4 or β-catenin upon AW treatment (Fig. 4*F*), depletion of either Smad2 or β-catenin affected FOXH1 binding on ME genes (Fig. 4*G*), suggesting that both Smad2 and β-catenin are important for FOXH1 recruitment.

Figure 1. Smad2 and β-catenin are enriched in the open chromatin regions of ME genes upon Activin and Wnt treatment. *A*, H1 cells were treated with 25 ng/ml of Activin A, 25 ng/ml of Wnt3a, or both (AW) for 6 h and then harvested for ATAC-seq. The data were measured through Pearson correlation analysis by $\log_2$ (RPKM). *B*, after peak calling analysis, the percentage of open signals in each group is shown as a *bar chart*. A random set of peaks that match the lengths of individual ATAC-seq peaks on the same chromosomes were used as a control. *C*, expression heatmap of 4 different groups was presented, and the enrichment was calculated by $\log_2$ (FPKM). *D*, H1 cells were treated with 25 ng/ml of Activin A, Wnt3a, or AW for 6 h before being harvested for ATAC-seq or ChIP-seq with antibodies against H3K27me3, H3K4me3, and Smad2, and snapshots of ME genes were shown. The ChIP-seq data of β-catenin, Pol2, and FOXH1 from GSE64758 and GSE29422 were also analyzed. Treatment conditions for β-catenin ChIP-seq were Wnt3a (200 ng/ml) and Pol2 ChIP-seq were Activin A (100 ng/ml) and Wnt3a (200 ng/ml). *E*, ChIP-qPCR analysis on ME marker genes was performed after H1 cells were treated with AW for 6 h. The data are shown as mean ± S.E. by unpaired, two-tailed Student's *t* test ($n = 9$, including 3 biological replicates and 3 technical replicates). *, $p < 0.05$; **, $p < 0.01$; ***, $p < 0.001$. *F* and *G*, experiments were carried out as in *D*. Snapshots of pluripotent markers *OCT4* and *SALL4* (*F*), and ectoderm marker *SOX1*, trophoblast marker *CGA* (*G*) were shown.

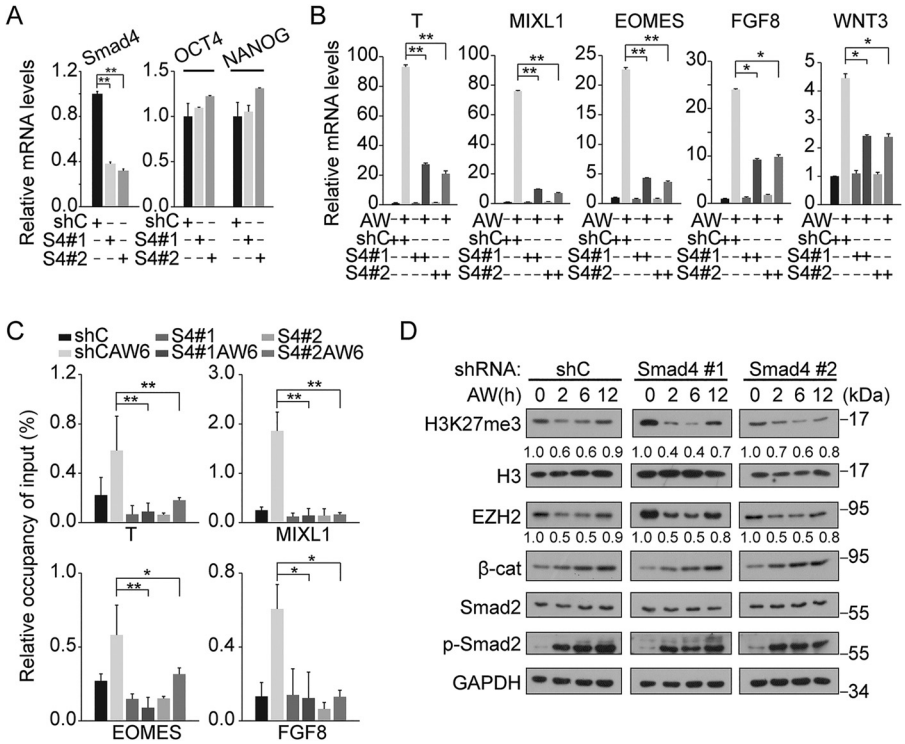

Figure 3. Smad4 is required for AW-induced Smad2 binding to ME gene promoters, but not for H3K27me3 reduction. *A*, H1 cells transfected with control or *Smad4* shRNA were harvested for qPCR. *B*, the expression of ME markers was detected by qPCR in *Smad4*-knockdown H1 cells. *C*, Smad2 enrichment on the promoters of *T*, *MIXL1*, *EOMES*, and *FGF8* was detected by ChIP-qPCR in *Smad4*-knockdown H1 cells after treatment with AW for 6 h. *D*, *Smad4*-knockdown H1 cells were treated with 25 ng/ml of AW for the indicated times before being harvested for histone extraction and then immunoblotting against H3K27me3, EZH2, β-catenin, Smad2, and phospho-Smad2. GAPDH served as loading control. The data are shown as mean ± S.E. by unpaired, two-tailed Student's *t* test ($n = 9$, including 3 biological replicates and 3 technical replicates). *, $p < 0.05$; **, $p < 0.01$; ***, $p < 0.001$.

HAS2 and ALDH3A2 act downstream of Activin and Wnt signaling to promote ME differentiation

To identify the downstream mediators, we picked up 33 genes from our previous RNA-seq data that were significantly up-regulated by Activin and Wnt along mesendoderm differentiation (Fig. 5*A*, Table S2) (11) and found that *HAS2* and *ALDH3A2* had strong open chromatin signals with enrichment of FOXH1, Smad2, and β-catenin (Fig. 5*B*). Although there are three hyaluronan synthase genes, *HAS1*, *HAS2*, and *HAS3* (38), only *HAS2* was co-regulated by AW treatment (Fig. 5*C*). *HAS2* has been shown to function in hESC differentiation to primitive endoderm and mesoderm (39). Aldehyde dehydrogenase 3 family member A2 (ALDH3A2), enriched in skin, adrenal, kidney, and liver, plays a major role in fatty acid metabolism, and its mutations are associated with Sjogren-Larsson syndrome (40). To confirm the importance of Activin and Wnt signaling in the expression of *HAS2* and *ALDH3A2*, we examined their expression in *Smad2* or *β-catenin*-knockdown H1 cells. The expression of *HAS2* and *ALDH3A2* was induced by AW treatment, but apparently attenuated in the knockdown cells (Fig. 5*D*). Depletion of *FOXH1* had a similar effect. Interestingly, *FOXH1* knockdown also significantly impaired the recruitment of Smad2 and β-catenin to the *HAS2* and *ALDH3A2* genes (Fig. 5*E*). Taken together, our results indicate that Smad2, β-catenin, and FOXH1 cooperatively regulate the expression of *HAS2* and *ALDH3A2*.

To explore the function of *HAS2* and *ALDH3A2* in ME specification, we generated knockdown H1 cells (Fig. 5*F*). As shown in Fig. 5*G*, knockdown of *HAS2* strongly attenuated the AW-induced expression of ME markers. *ALDH3A2* also had a similar effect albeit to a lesser extent. Aldehyde dehydrogenases are critical in fatty acid metabolism, especially retinoic acid (RA) production (41). To investigate the possible involvement of RA in AW-induced ME specification, we applied different doses of retinoic acid together with Activin A and Wnt3a for 24 h and found that RA had no effect on the AW-induced expression of ME markers in WT H1 cells (Fig. 5*H*). However, 2 nM RA could rescue the expression of *T* and *MIXL1* in *ALDH3A2* knockdown cells (Fig. 5*I*). Therefore, *ALDH3A2* may modulate ME differentiation through its metabolic product RA. These data together indicate the important function of *HAS2* and *ALDH3A2* in ME specification.

To further confirm the significance of AW-induced target genes in mesoderm and endoderm specification, we conducted a long differentiation assay after AW-induced ME differentiation: 25 ng/ml AW for 96 h for the endoderm lineage and AW for 48 h followed by BMP4 and FGF2 treatment for another 48 h for the mesoderm lineage. Our results revealed that the expression of both mesendoderm marker (*T*) and endoderm markers (*FOXA2*, *SOX17*) was attenuated after knockdown of *Smad2*, *β-catenin*, *HAS2*, or *ALDH3A2* (Fig. 6*A*). Furthermore, the impaired expression of mesoderm markers *PDGFRα* and *SOX9* was also observed in knockdown cells (Fig. 6*B*). Consistent with the mRNA levels, we conducted immunofluorescence experiments and observed that the expression of T, FOXA2, and SOX9 were dampened in knockdown cells (Fig. 6, *C–E*). Taken

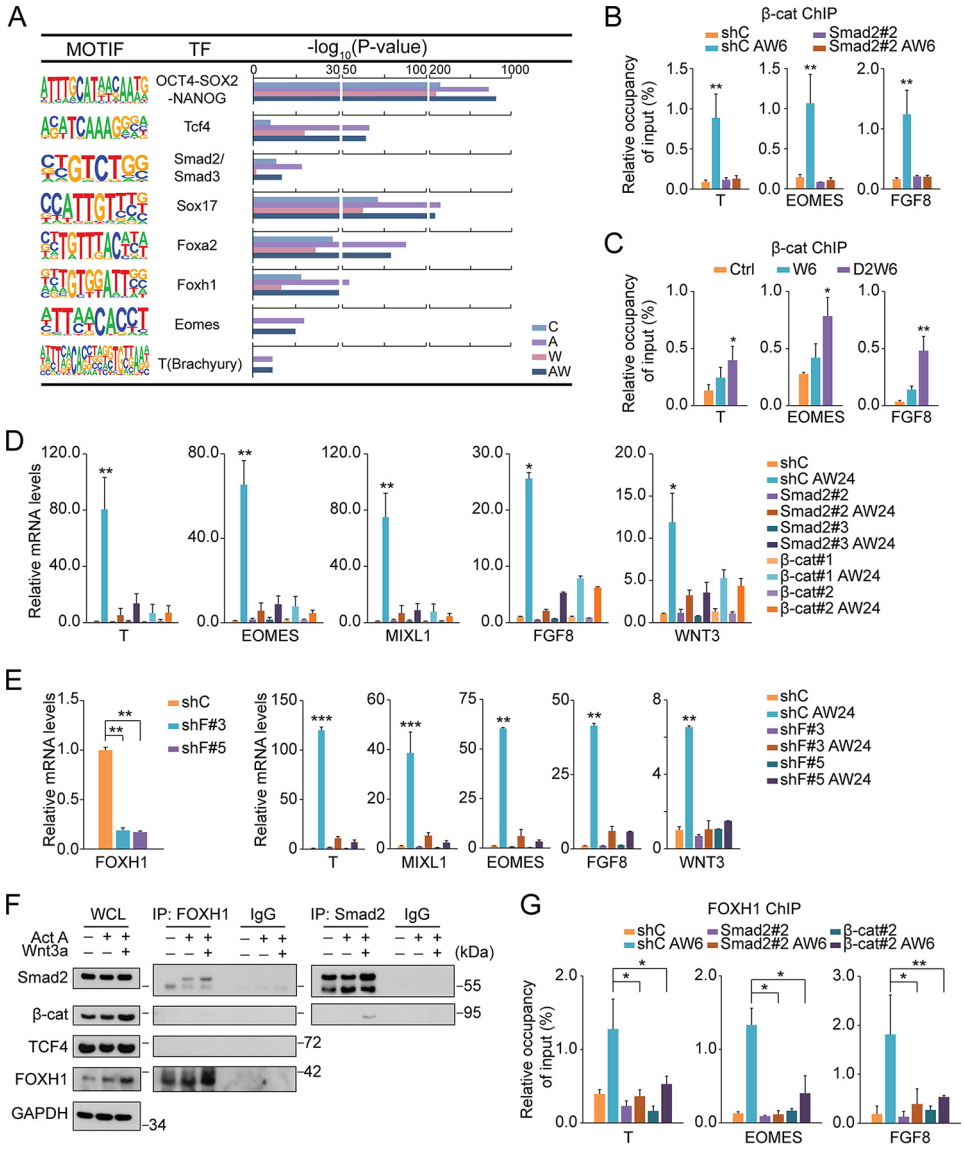

Figure 4. Smad2 and β-catenin cooperate with FOXH1 to induce ME differentiation. *A*, after ATAC-seq peak calling analysis, motif analysis was conducted by HOMER, and some of the transcription factors related with mesendoderm/endoderm development are listed. *B*, *Smad2*-knockdown H1 cells were treated with AW for 6 h and harvested for β-catenin ChIP-qPCR to analyze its binding on ME gene promoters. *C*, H1 cells pretreated with 10 ng/ml of DZNep for 2 h (*D2*) were treated with 25 ng/ml of Wnt3a for 6 h, and then harvested for β-catenin ChIP-qPCR to analyze its binding on ME marker genes. *D*, *Smad2* or *β-catenin*-knockdown H1 cells were treated with AW for 24 h and harvested for qPCR to assess ME gene expression. *E*, H1 cells transfected with control or *FOXH1* shRNA were harvested for qPCR. ME marker expression was detected in *FOXH1*-knockdown H1 cells after treatment with AW for 24 h. *F*, H1 cells were treated with 25 ng/ml of Activin A, Wnt3a, or AW for 6 h before being harvested for immunoprecipitation followed by immunoblotting. GAPDH served as loading control. *G*, FOXH1 ChIP-qPCR was conducted in *Smad2*- or *β-catenin*-knockdown H1 cells, and FOXH1 enrichment was detected on the promoters of *T*, *EOMES*, and *FGF8*. The data are shown as mean ± S.E. by unpaired, two-tailed Student's *t* test ($n = 9$, including 3 biological replicates and 3 technical replicates). *, $p < 0.05$; **, $p < 0.01$; ***, $p < 0.001$.

together, these results further demonstrate the important roles of Smad2, β-catenin, *HAS2*, and *ALDH3A2* in the commitment of mesendoderm and the following lineages.

Discussion

Our results highlight an important role of Activin/Smad2 signaling at the early stages of ME differentiation through reducing histone modification H3K27me3 without changing the global open chromatin pattern, increasing accessibility at that region. By cooperating with β-catenin and FOXH1 on accessible chromatin, Smad2 up-regulates the expression of ME marker genes, including HAS2 and ALDH3A2 (Fig. 6*F*).

H3K27me3 is a marker for chromatin accessibility, and generally a low level of H3K27me3 indicates a more accessible chromatin state for gene transcription (22–24). H3K27me3 levels are the result of balance between the methyltransferase PRC2 and the demethylases JMJD3 and UTX (22). JMJD3 and UTX have been shown to play an important role in endoderm differentiation from human ESCs (42), but our previous data suggest that JMJD3 and UTX may not be involved in H3K27me3 reduction in the early stages of AW-induced ME differentiation (11). Instead, we found that Activin reduces the H3K27me3 levels and the PRC2 methyltransferase EZH2 with a similar pattern, and their decrease depends on Smad2, but not Smad4 or Wnt/β-catenin. Furthermore, Activin/Smad2 promotes EZH2 polyubiquitination and degradation via the proteasome pathway. It has been reported that EZH2 down-regulation enhances neuron differentiation of human mesenchymal

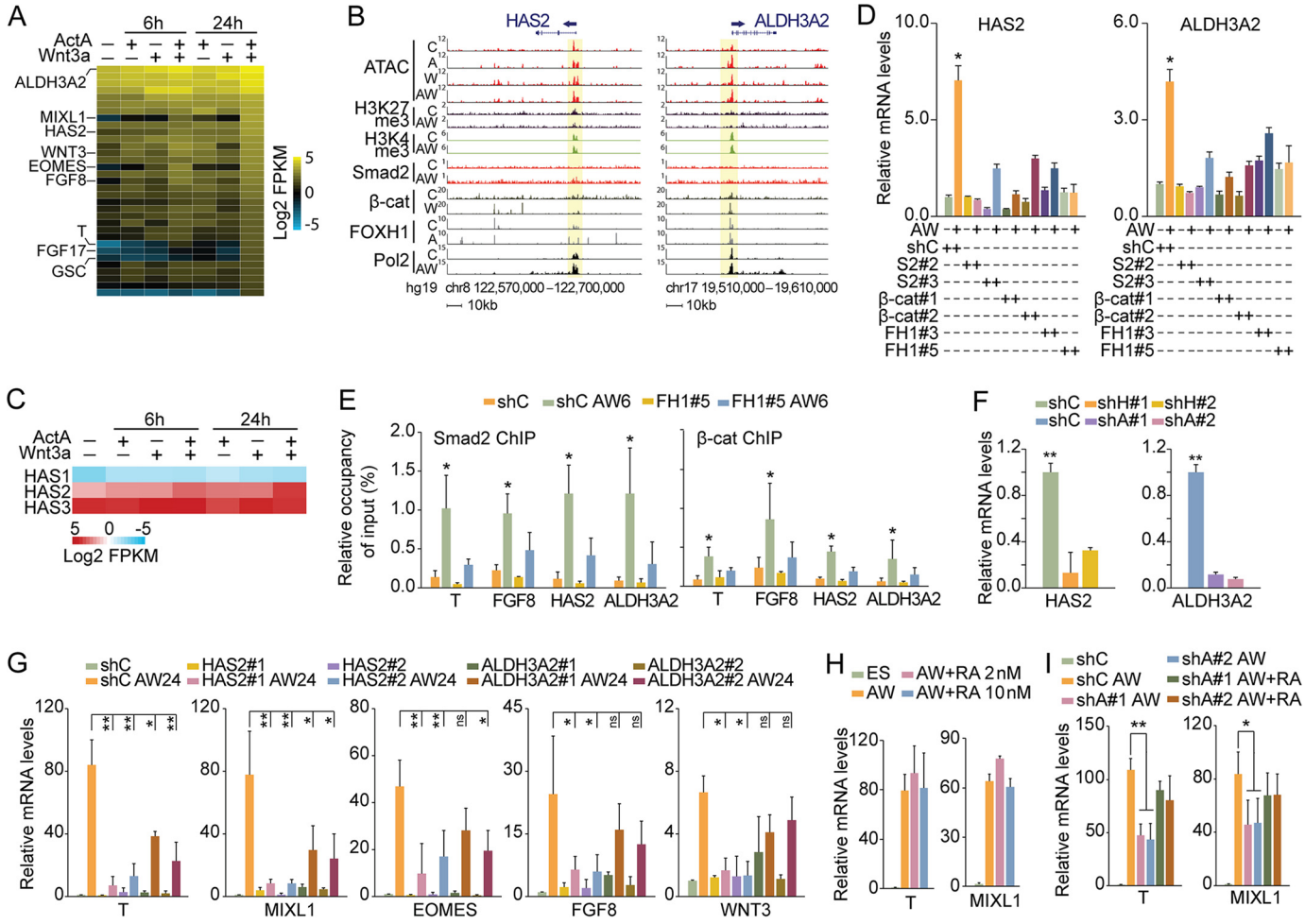

Figure 5. HAS2 and ALDH3A2 are important for ME differentiation. *A*, expression heatmap of Activin/Wnt-coregulated genes was presented, and the enrichment was calculated by $\log_2$ (RPKM). *B*, snapshots of open chromatin, H3K27me3, H3K4me3, and binding of Smad2, β-catenin, FOXH1, and Pol2 on the promoters of *HAS2* and *ALDH3A2* were shown. *C*, the expression profile of *HAS1*, *HAS2*, and *HAS3* was presented, and the enrichment was calculated by $\log_2$ (RPKM). *D*, the expression of *HAS2* and *ALDH3A2* was detected in *Smad2*, *β-catenin*, or *FOXH1*-knockdown H1 after AW treatment for 24 h. *E*, Smad2 and β-catenin ChIP-qPCR were conducted in *FOXH1*-knockdown H1 cells, and enrichment was detected on the promoters of *T*, *FGF8*, *HAS2*, and *ALDH3A2*. *F*, knockdown efficiency of *HAS2* and *ALDH3A2* was measured by qPCR. *G*, *HAS2* or *ALDH3A2*-knockdown H1 cells were treated with AW for 24 h and harvested for qPCR to assess ME gene expression. *H*, H1 cells were treated with retinoic acid together with AW for 24 h and then harvested for qPCR. *I*, H1 cells were transfected with control or *ALDH3A2* shRNA and treated with AW and 2 nM retinoic acid for 24 h and then harvested for qPCR. The data are shown as mean ± S.E. by unpaired, two-tailed Student's *t* test ($n = 9$, including 3 biological replicates and 3 technical replicates). *, $p < 0.05$; **, $p < 0.01$; ***, $p < 0.001$.

stem cells and Smurf2 is responsible for the EZH2 decrease (43). EZH2 knockout led to H3K27me3 decrease and reduced self-renewal and proliferation of human embryonic stem cells and their full differentiation into mature specialized tissues (29), indicating the complex role of EZH2 in cell lineage commitment.

FOXH1 was identified as a Smad2 DNA-binding partner to mediate Activin signaling during early embryo patterning (33, 34, 44). *Foxh1* null mice show defects in development of the anterior primitive streak, axial patterning, and endoderm formation (36). *FOXH1* is also involved in endoderm specification of human ESCs (37). It has been demonstrated that Activin signaling disrupts the repression of *FOXH1* by the NuRD corepressor complex, resulting in the cooperative action of FOXH1 and Smad2 to activate ME genes (45). Our data indicate that AW treatment enhances FOXH1 binding to ME gene promoters, and this recruitment needs both Smad2 and β-catenin. In agreement with this, knockdown of β-catenin greatly reduces *FOXH1* promotion of cell proliferation and invasion (46).

Our data showed that the hyaluronan synthase *HAS2* is induced by AW treatment and mediates ME specification, which is consistent with the demonstrated role of HAS2 in the formation of endoderm (39, 47). The aldehyde dehydrogenases are critical in fatty acid metabolism, especially the retinoic acid production (41), and retinoic acid can cooperate with various signals to promote lineage specification and tissue development (48, 49). Our data also suggest that *ALDH3A2*-mediated retinoic acid generation is important for AW-induced ME specification. Therefore, our work indicates that Activin/Smad2 signaling controls the epigenetic modifications and by cooperating with Wnt/β-catenin signaling, regulate the expression of ME-specifying genes.

Experimental procedures

Cell culture and differentiation of human ESCs

H1 human embryonic stem cells (WiCell, 12-W0296) were cultured on feeder cells with DMEM/F-12 (Gibco) supplemented with 20% knockout serum replacement (Gibco), 1 mM

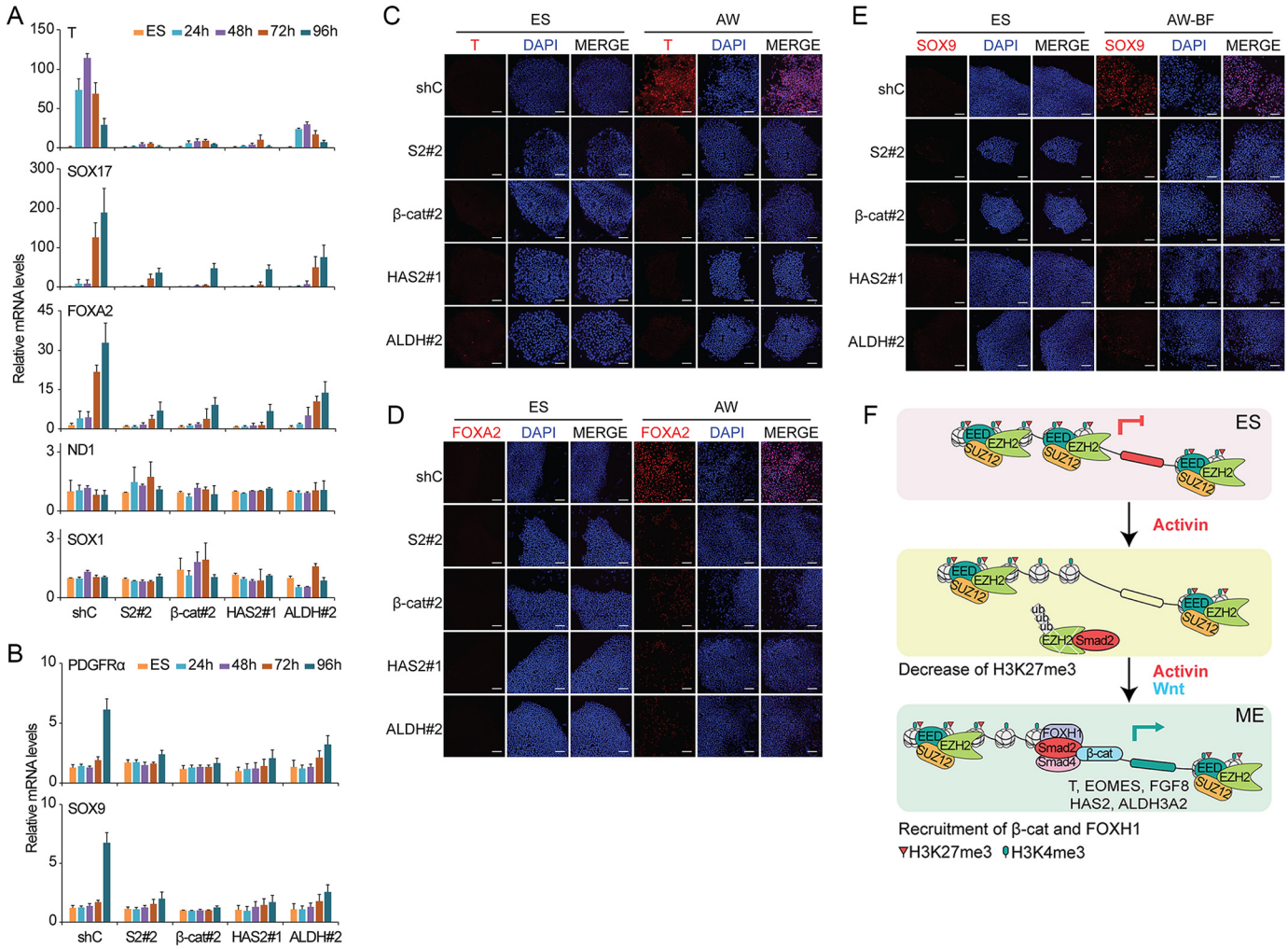

Figure 6. The Activin/Smad2- and Wnt/β-catenin-regulated expression of HAS2 and ALDH3A2 is important for mesoderm and endoderm differentiation. *A*, H1 cells expressing control shRNA or *Smad2*, *β-catenin*, *HAS2*, or *ALDH3A2* shRNA were treated with AW (25 ng/ml each) for the indicated times and then harvested for qPCR to assess the expression of ME (*T*), endoderm (*SOX17*, *FOXA2*), and ectoderm (*SOX1*, *ND1*) genes. *B*, H1 cells expressing control shRNA or *Smad2*, *β-catenin*, *HAS2*, or *ALDH3A2* shRNA were treated with AW (25 ng/ml) for 48 h, then replaced with 20 ng/ml of BMP4 and 40 ng/ml of FGF2 for another 48 h and harvested by qPCR to assess the expression of the mesoderm genes *PDGFRα* and *SOX9*. The data are shown as mean ± S.E. ($n = 9$, including 3 biological replicates and 3 technical replicates). *C*, H1 cells expressing control shRNA or Smad2, *β-catenin*, *HAS2*, or *ALDH3A2* shRNA were cultured on Matrigel-coated plates and treated with 25 ng/ml of Activin A and 25 ng/ml of Wnt3a for 48 h. Anti-T immunofluorescence (1:100) was conducted. *D*, H1 cells were treated with 25 ng/ml of Activin A and 25 ng/ml of Wnt3a for 96 h. Anti-FOXA2 (1:100) immunofluorescence was conducted. *E*, H1 cells were treated with 25 ng/ml of Activin A and 25 ng/ml Wnt3a for 48 h, then replaced with 20 ng/ml of BMP4 and 40 ng/ml of FGF2 for another 48 h. Anti-SOX9 immunofluorescence (1:100) was conducted. The nucleus was counterstained with DAPI. *Scale bar*, 100 μm. *F*, schematic model. In the ES stage, the regulatory regions of lineage markers maintain a poised state with both H3K27me3 and H3K4me3 modifications. Upon AW treatment, Smad2 reduces H3K27me3 through EZH2 degradation, and then with the recruitment of β-catenin and FOXH1, together they cooperate to activate transcription of ME genes.

L-glutamine, 0.1 mM nonessential amino acids, 0.1 mM β-mercaptoethanol, and 10 ng/ml of recombinant human bFGF. Although for feeder-free culture, H1 cells were maintained on a Matrigel (BD Biosciences)-coated plate with N2B27 medium (DMEM/F-12 supplemented with N2, B27, 1 mM L-glutamine, 0.1 mM nonessential amino acids, 0.1 mM β-mercaptoethanol, and 20 ng/ml of recombinant human bFGF) (Table S3). For mesendoderm differentiation, H1 cells were maintained on a Matrigel-coated plate with N2B27/bFGF medium to about 50–60% confluence, and then differentiation was conducted in B27 medium (DMEM/F-12, B27, 1 mM L-glutamine, 0.1 mM nonessential amino acids) supplemented with Activin A (25 ng/ml), Wnt3a (25 ng/ml), or Activin A plus Wnt3a (25 ng/ml for each). For mesoderm differentiation, H1 cells were cultured in B27 medium (DMEM/F-12, B27, 1 mM L-glutamine, 0.1 mM nonessential amino acids) with AW (25 ng/ml for each) for the first 48 h and then replaced with 20 ng/ml of BMP4 and 40 ng/ml of FGF2 for another 48 h.

shRNA-mediated knockdown

All shRNA plasmids were obtained from the Sigma TRC shRNA library (Table S4), and a nontargeting nucleotide plasmid served as control. shRNAs were packed into lentivirus following the instruction. H1 cells were cultured in a feeder-free condition and infected with shRNA lentiviral supernatant. Then puromycin (1 μg/ml; Invitrogen) was added into culture medium for 3–5 days to select stable knockdown cells.

Histone extraction

H1 cells were lysed with TEB buffer (PBS containing 0.5% Triton X-100, 2 mM phenylmethylsulfonyl fluoride, 0.02%

NaN_3) added to the proteinase inhibitor mixture (Roche Applied Science) at 4 °C for 15 min and then centrifuged at 2000 rpm for 10 min. After removing the supernatant and washing the pellets twice with 500 μl of TEB buffer with proteinase inhibitors at 4 °C, the pellets were suspended with 0.2 N HCl and incubated overnight at 4 °C. Then histones were precipitated with 100% TCA at a final concentration of 33% and incubated for 1–2 h on ice. After centrifugation at 4 °C for 10 min, the supernatant was discarded, and the histone pellets were washed with ice-cold acetone, the pellets were air-dried for 5 min and dissolved with a suitable volume of 150 mM NaCl.

ATAC-seq library preparation, sequencing, and data processing

The ATAC-seq libraries of hESCs were prepared as previously described with minor modifications (24). Briefly, samples were lysed in lysis buffer (10 mM Tris-HCl (pH 7.4), 10 mM NaCl, 3 mM $MgCl_2$, and 0.5% Nonidet P-40) for 10 min on ice. Immediately after lysis, cells were then incubated with the Tn5 transposome and tagmentation buffer at 37 °C for 30 min (Vazyme Biotech TD502), and the stop buffer was added directly into the reaction to end the tagmentation. PCR was performed to amplify the library for 12 cycles using the following PCR conditions: 72 °C for 3 min; 98 °C for 30 s; and thermocycling at 98 °C for 15 s, 60 °C for 30 s and 72 °C for 3 min; followed by 72 °C 5 min. After the PCR, libraries were purified with the 1.5× AMPure (Beckman) beads. The ATAC-seq library was subjected to sequencing on HiSeq2500 or Xten (Illumina) according to the manufacturer's instruction. All ATAC-seq reads were first aligned to hg19 using Bowtie2 (version 2.2.2). The paired-end ATAC-seq reads were aligned with the parameters: -t -q -N1 -L25 -X2000 no-mixed no-discordant. All unmapped reads, nonuniquely mapped reads, and PCR duplicates were removed. For downstream analysis, we normalized the read counts by computing the numbers of reads per kilobase of bin per million of reads (RPKM). To visualize the ATAC-seq signal in the UCSC genome browser, we extended each read by 250 bp and counted the coverage for each base. All ATAC-seq peaks were called by MACS (version 1.4.2) with the parameters -nolambda -nomodel. Motif analysis was conducted by HOMER (hypergeometric optimization of motif enrichment) following the instructions.

RNA-seq data processing

Paired end reads were first trimmed of the first 15 bp from each end and then mapped to the human genome (hg19) using STAR (version 2.4.0d). Gene expression was estimated and normalized with Cuffnorm from the Cufflinks package (version 2.2.1) into an FPKM matrix using default parameters, and the expression matrix was $\log_2$-transformed.

Quantitative RT-PCR, ChIP, immunoprecipitation, immunoblotting, and immunofluorescence

These were performed as previously described (11). The primers for qPCR and ChIP-qPCR are listed in Tables S5 and S6. Antibodies used in this study are summarized in Table S3.

Statistical analysis

All of the values are shown as mean ± S.E. with a two-way analysis of variance test. The significance between groups was determined by Student's *t* test. *, $p < 0.05$; **, $p < 0.01$; ***, $p < 0.001$.

Author contributions—X. X., L. W., W. X., and Y.-G. C. conceptualization; X. X., L. W., B. L., and Y.-G. C. data curation; X. X., L. W., B. L., W. X., and Y.-G. C. formal analysis; X. X., L. W., and B. L. investigation; X. X., L. W., and B. L. methodology; X. X. and Y.-G. C. writing-original draft; W. X. and Y.-G. C. supervision; W. X. and Y.-G. C. writing-review and editing; Y.-G. C. funding acquisition; Y.-G. C. project administration.

Acknowledgments—We are grateful to Dr. Teng Fei for critical reading of the manuscript and Dr. Qiaoran Xi for experimental suggestions.

References

1. Pera, M. F., and Tam, P. P. (2010) Extrinsic regulation of pluripotent stem cells. *Nature* **465,** 713–720 CrossRef Medline
2. Young, R. A. (2011) Control of the embryonic stem cell state. *Cell* **144,** 940–954 CrossRef Medline
3. Wang, L., and Chen, Y. G. (2016) Signaling control of differentiation of embryonic stem cells toward mesendoderm. *J. Mol. Biol.* **428,** 1409–1422 CrossRef Medline
4. Reissmann, E., Jörnvall, H., Blokzijl, A., Andersson, O., Chang, C., Minchiotti, G., Persico, M. G., Ibáñez, C. F., and Brivanlou, A. H. (2001) The orphan receptor ALK7 and the Activin receptor ALK4 mediate signaling by Nodal proteins during vertebrate development. *Genes Dev.* **15,** 2010–2022 CrossRef Medline
5. Kunwar, P. S., Zimmerman, S., Bennett, J. T., Chen, Y., Whitman, M., and Schier, A. F. (2003) Mixer/Bon and FoxH1/Sur have overlapping and divergent roles in Nodal signaling and mesendoderm induction. *Development* **130,** 5589–5599 CrossRef Medline
6. Gaarenstroom, T., and Hill, C. S. (2014) TGF-beta signaling to chromatin: how Smads regulate transcription during self-renewal and differentiation. *Semin. Cell Dev. Biol.* **32,** 107–118 CrossRef Medline
7. Muñoz-Descalzo, S., Hadjantonakis, A. K., and Arias, A. M. (2015) Wnt/ss-catenin signalling and the dynamics of fate decisions in early mouse embryos and embryonic stem (ES) cells. *Semin. Cell Dev. Biol.* **47,** 101–109 Medline
8. Itoh, F., Watabe, T., and Miyazono, K. (2014) Roles of TGF-β family signals in the fate determination of pluripotent stem cells. *Semin. Cell Dev. Biol.* **32,** 98–106 CrossRef Medline
9. Funa, N. S., Schachter Karen, A., Lerdrup, M., Ekberg, J., Hess, K., Dietrich, N., Honoré, C., Hansen, K., and Semb, H. (2015) β-Catenin regulates primitive streak induction through collaborative interactions with SMAD2/SMAD3 and OCT4. *Cell Stem Cell* **16,** 639–652 CrossRef Medline
10. Estarás, C., Benner, C., and Jones, K. A. (2015) SMADs and YAP compete to control elongation of β-catenin:LEF-1-recruited RNAPII during hESC differentiation. *Mol. Cell* **58,** 780–793 CrossRef Medline
11. Wang, L., Xu, X., Cao, Y., Li, Z., Cheng, H., Zhu, G., Duan, F., Na, J., Han, J. J., and Chen, Y. G. (2017) Activin/Smad2-induced histone H3 Lys-27 trimethylation (H3K27me3) reduction is crucial to initiate mesendoderm differentiation of human embryonic stem cells. *J. Biol. Chem.* **292,** 1339–1350 CrossRef Medline
12. Wang, Q., Zou, Y., Nowotschin, S., Kim, S. Y., Li, Q. V., Soh, C. L., Su, J., Zhang, C., Shu, W., Xi, Q., Huangfu, D., Hadjantonakis, A. K., and Massagué, J. (2017) The p53 family coordinates Wnt and Nodal inputs in mesendodermal differentiation of embryonic stem cells. *Cell Stem Cell* **20,** 70–86 CrossRef Medline
13. Bertero, A., Madrigal, P., Galli, A., Hubner, N. C., Moreno, I., Burks, D., Brown, S., Pedersen, R. A., Gaffney, D., Mendjan, S., Pauklin, S., and Val-

lier, L. (2015) Activin/nodal signaling and NANOG orchestrate human embryonic stem cell fate decisions by controlling the H3K4me3 chromatin mark. *Genes Dev.* **29,** 702–717 CrossRef Medline
14. Massagué, J., Seoane, J., and Wotton, D. (2005) Smad transcription factors. *Genes Dev.* **19,** 2783–2810 CrossRef Medline
15. Feng, X. H., and Derynck, R. (2005) Specificity and versatility in TGF-β signaling through Smads. *Annu. Rev. Cell Dev. Biol.* **21,** 659–693 CrossRef Medline
16. Hill, C. S. (2016) Transcriptional control by the SMADs. *Cold Spring Harb. Perspect. Biol.* **8,** a022079 CrossRef Medline
17. Heldin, C. H., Miyazono, K., and ten Dijke, P. (1997) TGF-β signalling from cell membrane to nucleus through SMAD proteins. *Nature* **390,** 465–471 CrossRef Medline
18. Lindsley, R. C., Gill, J. G., Kyba, M., Murphy, T. L., and Murphy, K. M. (2006) Canonical Wnt signaling is required for development of embryonic stem cell-derived mesoderm. *Development* **133,** 3787–3796 CrossRef Medline
19. Clevers, H., Loh, K. M., and Nusse, R. (2014) Stem cell signaling. An integral program for tissue renewal and regeneration: Wnt signaling and stem cell control. *Science* **346,** 1248012 CrossRef Medline
20. Li, M., Liu, G. H., and Izpisua Belmonte, J. C. (2012) Navigating the epigenetic landscape of pluripotent stem cells. *Nat. Rev. Mol. Cell Biol.* **13,** 524–535 CrossRef Medline
21. Pan, M. R., Hsu, M. C., Chen, L. T., and Hung, W. C. (2018) Orchestration of H3K27 methylation: mechanisms and therapeutic implication. *Cell Mol. Life Sci.* **75,** 209–223 CrossRef Medline
22. Kimura, H. (2013) Histone modifications for human epigenome analysis. *J. Hum. Genet.* **58,** 439–445 CrossRef Medline
23. Dixon, J. R., Jung, I., Selvaraj, S., Shen, Y., Antosiewicz-Bourget, J. E., Lee, A. Y., Ye, Z., Kim, A., Rajagopal, N., Xie, W., Diao, Y., Liang, J., Zhao, H., Lobanenkov, V. V., Ecker, J. R., Thomson, J. A., and Ren, B. (2015) Chromatin architecture reorganization during stem cell differentiation. *Nature* **518,** 331–336 CrossRef Medline
24. Wu, J., Huang, B., Chen, H., Yin, Q., Liu, Y., Xiang, Y., Zhang, B., Liu, B., Wang, Q., Xia, W., Li, W., Li, Y., Ma, J., Peng, X., Zheng, H., *et al.* (2016) The landscape of accessible chromatin in mammalian preimplantation embryos. *Nature* **534,** 652–657 CrossRef Medline
25. Voigt, P., Tee, W. W., and Reinberg, D. (2013) A double take on bivalent promoters. *Genes Dev.* **27,** 1318–1338 CrossRef Medline
26. Martin, C., and Zhang, Y. (2005) The diverse functions of histone lysine methylation. *Nat. Rev. Mol. Cell Biol.* **6,** 838–849 CrossRef Medline
27. Loh, K. M., Chen, A., Koh, P. W., Deng, T. Z., Sinha, R., Tsai, J. M., Barkal, A. A., Shen, K. Y., Jain, R., Morganti, R. M., Shyh-Chang, N., Fernhoff, N. B., George, B. M., Wernig, G., Salomon, R. E. A., *et al.* (2016) Mapping the pairwise choices leading from pluripotency to human bone, heart, and other mesoderm cell types. *Cell* **166,** 451–467 CrossRef Medline
28. Laugesen, A., and Helin, K. (2014) Chromatin repressive complexes in stem cells, development, and cancer. *Cell Stem Cell* **14,** 735–751 CrossRef Medline
29. Collinson, A., Collier, A. J., Morgan, N. P., Sienerth, A. R., Chandra, T., Andrews, S., and Rugg-Gunn, P. J. (2016) Deletion of the Polycomb-group protein EZH2 leads to compromised self-renewal and differentiation defects in human embryonic stem cells. *Cell Rep.* **17,** 2700–2714 CrossRef Medline
30. Lolas, M., Valenzuela, P. D., Tjian, R., and Liu, Z. (2014) Charting Brachyury-mediated developmental pathways during early mouse embryogenesis. *Proc. Natl. Acad. Sci. U.S.A.* **111,** 4478–4483 CrossRef Medline
31. Teo, A. K., Arnold, S. J., Trotter, M. W., Brown, S., Ang, L. T., Chng, Z., Robertson, E. J., Dunn, N. R., and Vallier, L. (2011) Pluripotency factors regulate definitive endoderm specification through eomesodermin. *Genes Dev.* **25,** 238–250 CrossRef Medline
32. Zhou, S., Zawel, L., Lengauer, C., Kinzler, K. W., and Vogelstein, B. (1998) Characterization of human FAST-1, a TGFβ and activin signal transducer. *Mol. Cell* **2,** 121–127 CrossRef Medline
33. Attisano, L., Silvestri, C., Izzi, L., and Labbé, E. (2001) The transcriptional role of Smads and FAST (FoxH1) in TGFβ and activin signalling. *Mol. Cell Endocrinol.* **180,** 3–11 CrossRef Medline
34. Chen, X., Weisberg, E., Fridmacher, V., Watanabe, M., Naco, G., and Whitman, M. (1997) Smad4 and FAST-1 in the assembly of activin-responsive factor. *Nature* **389,** 85–89 CrossRef Medline
35. Liu, F., Pouponnot, C., and Massagué, J. (1997) Dual role of the Smad4/DPC4 tumor suppressor in TGFβ-inducible transcriptional complexes. *Genes Dev.* **11,** 3157–3167 CrossRef Medline
36. Hoodless, P. A., Pye, M., Chazaud, C., Labbé, E., Attisano, L., Rossant, J., and Wrana, J. L. (2001) FoxH1 (Fast) functions to specify the anterior primitive streak in the mouse. *Genes Dev.* **15,** 1257–1271 CrossRef Medline
37. Kim, S. W., Yoon, S. J., Chuong, E., Oyolu, C., Wills, A. E., Gupta, R., and Baker, J. (2011) Chromatin and transcriptional signatures for Nodal signaling during endoderm formation in hESCs. *Dev. Biol.* **357,** 492–504 CrossRef Medline
38. Spicer, A. P., Augustine, M. L., and McDonald, J. A. (1996) Molecular cloning and characterization of a putative mouse hyaluronan synthase. *J. Biol. Chem.* **271,** 23400–23406 CrossRef Medline
39. Choudhary, M., Zhang, X., Stojkovic, P., Hyslop, L., Anyfantis, G., Herbert, M., Murdoch, A. P., Stojkovic, M., and Lako, M. (2007) Putative role of hyaluronan and its related genes, *HAS2* and *RHAMM*, in human early preimplantation embryogenesis and embryonic stem cell characterization. *Stem Cells* **25,** 3045–3057 CrossRef Medline
40. Keller, M. A., Zander, U., Fuchs, J. E., Kreutz, C., Watschinger, K., Mueller, T., Golderer, G., Liedl, K. R., Ralser, M., Kräutler, B., Werner, E. R., and Marquez, J. A. (2014) A gatekeeper helix determines the substrate specificity of Sjogren-Larsson syndrome enzyme fatty aldehyde dehydrogenase. *Nat. Commun.* **5,** 4439 CrossRef Medline
41. Chen, M., Achkar, C., and Gudas, L. J. (1994) Enzymatic conversion of retinaldehyde to retinoic acid by cloned murine cytosolic and mitochondrial aldehyde dehydrogenases. *Mol. Pharmacol.* **46,** 88–96 Medline
42. Jiang, W., Wang, J., and Zhang, Y. (2013) Histone H3K27me3 demethylases KDM6A and KDM6B modulate definitive endoderm differentiation from human ESCs by regulating WNT signaling pathway. *Cell Res.* **23,** 122–130 CrossRef Medline
43. Yu, Y. L., Chou, R. H., Shyu, W. C., Hsieh, S. C., Wu, C. S., Chiang, S. Y., Chang, W. J., Chen, J. N., Tseng, Y. J., Lin, Y. H., Lee, W., Yeh, S. P., Hsu, J. L., Yang, C. C., Hung, S. C., and Hung, M. C. (2013) Smurf2-mediated degradation of EZH2 enhances neuron differentiation and improves functional recovery after ischaemic stroke. *EMBO Mol. Med.* **5,** 531–547 CrossRef Medline
44. Chen, X., Rubock, M. J., and Whitman, M. (1996) A transcriptional partner for MAD proteins in TGF-β signalling. *Nature* **383,** 691–696 CrossRef Medline
45. Beyer, T. A., Weiss, A., Khomchuk, Y., Huang, K., Ogunjimi, A. A., Varelas, X., and Wrana, J. L. (2013) Switch enhancers interpret TGF-β and Hippo signaling to control cell fate in human embryonic stem cells. *Cell Rep.* **5,** 1611–1624 CrossRef Medline
46. Liu, Y., Zhang, L., Meng, Y., and Huang, L. (2015) Benzyl isothiocyanate inhibits breast cancer cell tumorigenesis via repression of the FoxH1-mediated Wnt/β-catenin pathway. *Intl. J. Clin. Exp. Med.* **8,** 17601–17611 Medline
47. Camenisch, T. D., Spicer, A. P., Brehm-Gibson, T., Biesterfeldt, J., Augustine, M. L., Calabro, A., Jr., Kubalak, S., Klewer, S. E., and McDonald, J. A. (2000) Disruption of hyaluronan synthase-2 abrogates normal cardiac morphogenesis and hyaluronan-mediated transformation of epithelium to mesenchyme. *J. Clin. Invest.* **106,** 349–360 CrossRef Medline
48. Huang, W., Wang, G., Delaspre, F., Vitery Mdel, C., Beer, R. L., and Parsons, M. J. (2014) Retinoic acid plays an evolutionarily conserved and biphasic role in pancreas development. *Dev. Biol.* **394,** 83–93 CrossRef Medline
49. Davenport, C., Diekmann, U., Budde, I., Detering, N., and Naujok, O. (2016) Anterior-posterior patterning of definitive endoderm generated from human embryonic stem cells depends on the differential signaling of retinoic acid, Wnt-, and BMP-signaling. *Stem Cells* **34,** 2635–2647 CrossRef Medline